Acta Mechanica 161, 165–178 (2003)
DOI 10.1007/s00707-002-0993-y

Acta Mechanica
Printed in Austria

Peristaltic pumping of a micropolar fluid in a tube

D. Srinivasacharya, Warangal, India, and **M. Mishra** and **A. R. Rao**, Bangalore, India

Received June 20, 2002; revised October 23, 2002
Published online: April 17, 2003

Summary. Peristaltic transport of a micropolar fluid in a circular tube is studied under low Reynolds number and long wavelength approximations. The closed form solutions are obtained for velocity, microrotation components, as well as the stream function and they contain new additional parameters namely, N the coupling number and m the micropolar parameter. In the case of free pumping (pressure difference $\Delta p = 0$) the difference in pumping flux is observed to be very small for Newtonian and micropolar fluids but in the case of pumping ($\Delta p > 0$) the characteristics are significantly altered for different N and m. It is observed that the peristalsis in micropolar fluids works as a pump against a greater pressure rise compared with a Newtonian fluid. Streamline patterns which depict trapping phenomena are presented for different parameter ranges. The limit on the trapping of the center streamline is obtained. The effects of N and m on friction force for different Δp are discussed.

1 Introduction

Peristaltic flows are generated by the propagation of waves along the flexible walls of a channel or tube. The mechanism of peristalsis is involved in many biological and biomedical systems. The biological systems which involve peristalsis are urine transport from kidney to the bladder through the ureter, the transportation of chyme in the gastro-intestinal tract, the movement of spermatozoa in the ductus of efferentus of the male reproductive tract, movement of ovum in the fallopian tube, and vasomotion in small blood vessels. Peristaltic pumping is used in biomedical devices like heart lung machine to pump the blood. Peristaltic flows are also exploited in industrial pumping as they provide an efficient means for sanitary fluid transport. The industrial use of peristaltic pumping in roller/finger pumps is well known.

Several attempts, experimental and theoretical, have been made to understand the peristaltic transport in both mechanical and physiological situations under various approximations. Shapiro et al. [1] studied the peristaltic transport of Newtonian fluid using wave frame of reference under long wave length approximation and proved that the peristaltic wave movement of the walls really pump fluid against pressure rise even when the wave amplitude is small. They have also identified two important features of the peristaltic flows, trapping and reflux, in the context of physiological applications. Another mode to study the fluid mechanics of small amplitude peristaltic waves is by using laboratory frame of reference as given by Fung and Yih [2].

The behavior of most of the physiological fluids is known to be non–Newtonian. Hence in recent years the study of peristaltic transport of non–Newtonian fluids in channels or pipes has gained much attention. Several investigators [3], [4], [5], [6] have analyzed the peristaltic transport in physiological situations of interest. Most of these analytical studies use asymptotic expansions with small Reynolds number, wave number, amplitude ratio as the perturbation parameters. The model of micropolar fluid introduced by Eringen [7] represents fluids consisting of rigid, randomly oriented (or spherical) particles suspended in a viscous medium where the deformation of the particles is ignored. Micropolar fluids exhibit some microscopic effects arising from the local structure and micromotion of the fluid elements. Further, they can sustain couple stresses. The micropolar fluid is considered to model the blood flow in small arteries and the calculation of theoretical velocity profiles is observed in good agreement with the experimental data. A detailed survey of microcontinum fluid mechanics with several applications in physiological fluid flows has been presented by Ariman et al. [8]. Some interesting aspects of theory and applications of micropolar fluids are dealt in a recent book by Lukasazewicz [9].

Although, it is known that the fluids are suspensions of particulate matter in microscopically contiuous media, only a few recent studies [10], [11], [12] on the peristaltic transport have considered this aspect. Srivastava [10] has studied the peristlatic transport of couple stress fluid which takes particle size in to account. Philip and Chandra [11] have investigated the peristaltic transport of a simple microfluid which accounts for microrotation and microstretching of the particles contained in a small volume element, using long wavelength approximation. Girija Devi and Devanathan [12] have considered the peristaltic transport of micropolar fluid in a laboratory frame of reference. Under this frame of reference people have studied mainly the streamline pattern and velocity variations but not the pumping characteristics and the trapping associated with it. Recently, Muthu et al. [13] have studied the influence of wall properties on the peristaltic transport of a micropolar fluid and even in this paper the pumping characteristics are not discussed. It is speculated that blood flow in arteries exhibit peristalsis, Fung and Yih [2], Antanovskii and Ramkissoon [14] and it is well-known that blood behaves like a non-Newtonian fluid in microcirculation. Therefore, modelling blood by a micropolar fluid may be more appropriate.

In the present study, the peristaltic transport of an incompressible micropolar fluid is investigated. The analysis has been carried out in the wave frame of reference with long wavelength and zero Reynolds number assumption. The relationship between pressure gradient and time mean flow rate for various micropolar parameters and coupling numbers is obtained. The pumping characteristics and trapping phenomena are discussed in detail. Further, the friction force is analyzed for various micropolar parameters in all pumping ranges.

2 Mathematical formulation

Let (r', θ, x') be the cylindrical polar coordinate system with $r' = 0$ as the axis of symmetry of the tube. Consider the flow of an incompressible micropolar fluid in an axisymmetric tube of radius a, with a periodic peristaltic wave travelling along the wall with velocity c, wavelength λ, amplitude b and its instantaneous radius at any axial station x' is given by

$$r' = H\left(\frac{x' - ct}{\lambda}\right). \tag{2.1}$$

The flow is unsteady in the fixed frame (laboratory frame) of reference (r', θ, x'). However, in a coordinate system moving with the wave speed c (wave frame) (r, θ, x) the boundary shape is stationary. The transformation from fixed frame to wave frame is given by

$$r = r', \quad x = x' - ct, \quad V_x = V'_x - c, \quad \text{and} \quad V_r = V'_r, \tag{2.2}$$

where (V'_r, V'_x) and (V_r, V_x) are radial and axial velocity components in the stationary and moving coordinate system respectively. In the waveframe, the flow remains steady for a prescribed constant pressure gradient under the assumption that the tube length is an integral multiple of wavelength, see Shapiro et al. [1].

The equations governing the steady flow of an incompressible micropolar fluid in the absence of body force and body couple are:

$$\nabla \cdot \vec{V} = 0, \tag{2.3}$$

$$\rho(\vec{V} \cdot \nabla \vec{V}) = -\nabla p + k\nabla \times \vec{w} + (\mu + k)\nabla^2 \vec{V}, \tag{2.4}$$

$$\rho j(\vec{V} \cdot \nabla \vec{w}) = -2k\vec{w} + k\nabla \times \vec{V} - \gamma(\nabla \times \nabla \times \vec{w}) + (\alpha + \beta + \gamma)\nabla(\nabla \cdot \vec{w}), \tag{2.5}$$

where $\vec{V}$ is the velocity vector, $\vec{w}$ is the microrotation vector, p is the fluid pressure, ρ and j are the fluid density and microgyration parameters. Further, the material constants μ, k, α, β, and γ satisfy the following inequalities [7]:

$$2\mu + k \geq 0, \quad k \geq 0 \quad 3\alpha + \beta + \gamma \geq 0 \quad \gamma \geq |\beta|. \tag{2.6}$$

Since the flow is axisymmetric, all the variables are independent of θ. Hence, for this flow the velocity vector is given by $\vec{V} = (V_r, 0, V_x)$ and microrotation vector is $\vec{w} = (0, v_\theta, 0)$. Introducing the following nondimensional variables

$$\begin{aligned} &r = a\tilde{r}, \quad x = \lambda\tilde{x}, \quad V_x = c\tilde{V}_x, \quad V_r = \frac{ca}{\lambda}\tilde{V}_r, \quad v_\theta = \frac{c}{a}\tilde{v}_\theta, \\ &p = \frac{\lambda c \mu}{a^2}\tilde{p}, \quad t = \frac{\lambda}{c}\tilde{t}, \quad h = \frac{H}{a}, \quad j = \tilde{j}a^2, \end{aligned} \tag{2.7}$$

into Eqs. (2.3), (2.4), (2.5) and dropping the tildes, we get

$$\frac{\partial V_r}{\partial r} + \frac{V_r}{r} + \frac{\partial V_x}{\partial x} = 0, \tag{2.8}$$

$$\begin{aligned} &R_e\delta^3\left(V_r\frac{\partial V_r}{\partial r} + V_x\frac{\partial V_r}{\partial x}\right) \\ &\quad = -\frac{\partial p}{\partial r} + \frac{\delta^2}{1-N}\left(-N\frac{\partial v_\theta}{\partial x} + \frac{\partial^2 V_r}{\partial r^2} + \frac{1}{r}\frac{\partial V_r}{\partial r} - \frac{V_r}{r^2} + \delta^2\frac{\partial^2 V_r}{\partial x^2}\right), \end{aligned} \tag{2.9}$$

$$\begin{aligned} &R_e\delta\left(V_r\frac{\partial V_x}{\partial r} + V_x\frac{\partial V_x}{\partial x}\right) \\ &\quad = -\frac{\partial p}{\partial x} + \frac{1}{1-N}\left(\frac{N}{r}\frac{\partial(rv_\theta)}{\partial r} + \frac{\partial^2 V_x}{\partial r^2} + \frac{1}{r}\frac{\partial V_x}{\partial r} + \delta^2\frac{\partial^2 V_x}{\partial x^2}\right), \end{aligned} \tag{2.10}$$

$$\begin{aligned} &\frac{jR_e\delta(1-N)}{N}\left(V_r\frac{\partial v_\theta}{\partial r} + V_x\frac{\partial v_\theta}{\partial_x}\right) \\ &\quad = -2v_\theta + \left(\delta^2\frac{\partial V_r}{\partial x} - \frac{\partial V_x}{\partial r}\right) + \frac{2-N}{m^2}\left[\frac{\partial}{\partial r}\left(\frac{1}{r}\frac{\partial(rv_\theta)}{\partial r}\right) + \delta^2\frac{\partial^2 v_\theta}{\partial x^2}\right], \end{aligned} \tag{2.11}$$

where $\delta = a/\lambda, R_e = \rho ac/\mu$ is the Reynolds number, $N = k/(\mu + k)$ is the coupling number $(0 \leq N < 1)$ [15], and $m^2 = a^2k(2\mu + k)/(\gamma(\mu + k))$ is the micropolar parameter [7] and α, β do not appear in the governing equation as the microrotation vector $\vec{w}$ is solenoidal. In the limit

$k \to 0$ i.e., $N \to 0$, the Eqs. (2.9) (2.10) are uncoupled with (2.11) and they reduce to classical Navier-Stokes equations.

Under the assumptions of long wavelength $\delta \ll 1$ and neglecting inertia terms ($R_e = 0$), Eqs. (2.9), (2.10), (2.11) reduce to

$$\frac{\partial V_r}{\partial r} + \frac{V_r}{r} + \frac{\partial V_x}{\partial x} = 0, \tag{2.12}$$

$$\frac{\partial p}{\partial r} = 0, \tag{2.13}$$

$$\frac{N}{r}\frac{\partial (r v_\theta)}{\partial r} + \left(\frac{\partial^2 V_x}{\partial r^2} + \frac{1}{r}\frac{\partial V_x}{\partial r}\right) = (1-N)\frac{\partial p}{\partial x}, \tag{2.14}$$

$$2v_\theta + \left(\frac{\partial V_x}{\partial r}\right) - \frac{2-N}{m^2}\frac{\partial}{\partial r}\left(\frac{1}{r}\frac{\partial (r v_\theta)}{\partial r}\right) = 0. \tag{2.15}$$

The corresponding boundary conditions in the wave frame are

$$\frac{\partial V_x}{\partial r} = 0 \quad \text{at} \quad r = 0, \tag{2.16}$$

$$V_x = -1 \quad \text{at} \quad r = h, \tag{2.17}$$

$$v_\theta = 0 \quad \text{at} \quad r = h, \tag{2.18}$$

and

$$V_x \quad \text{and} \quad v_\theta \quad \text{are finite at} \quad r = 0. \tag{2.19}$$

In the limit of micropolar parameters tending to the proper values in Eqs. (2.12)–(2.19), we recover the governing equations for peristaltic flow given by Shapiro et al. [1].

3 Analytical solution

Noting the fact that p is a function of x only from (2.13), Eq. (2.14) is rewritten in the form:

$$\frac{\partial}{\partial r}\left[r\frac{\partial V_x}{\partial r} + N r v_\theta - (1-N)\frac{r^2}{2}\frac{dp}{dx}\right] = 0. \tag{3.1}$$

Integrating (3.1) and dividing by r, we get

$$\frac{\partial V_x}{\partial r} = (1-N)\left[\frac{r}{2}\frac{dp}{dx} + \frac{C_1(x)}{r}\right] - N v_\theta. \tag{3.2}$$

Using (3.2) in (2.15), we get

$$\frac{\partial^2 v_\theta}{\partial r^2} + \frac{1}{r}\frac{\partial v_\theta}{\partial r} - (m^2 + \frac{1}{r^2})v_\theta = \frac{m^2(1-N)}{2-N}\left[\frac{r}{2}\frac{dp}{dx} + \frac{C_1(x)}{r}\right]. \tag{3.3}$$

The general solution of (3.3) is

$$v_\theta = C_2(x)I_1(mr) + C_3(x)K_1(mr) - \frac{1-N}{(2-N)}\left[\frac{r}{2}\frac{dp}{dx} + \frac{C_1(x)}{r}\right], \tag{3.4}$$

where $I_1(mr)$ and $K_1(mr)$ are modified Bessel functions of first order, first and second kind, respectively. Substituting (3.4) into (3.2) and integrating we obtain:

$$V_x = \frac{N}{m}[-C_2(x)I_0(mr) + C_3(x)K_0(mr)] + \frac{1-N}{(2-N)}\left(\frac{r^2}{2}\frac{dp}{dx} + 2C_1(x)\log r\right) + C_4(x), \tag{3.5}$$

where I_0 and K_0 are modified Bessel functions of zeroth-order. The arbitrary functions $C_1(x) = C_3(x) = 0$ in (3.4) as we require v_θ to be finite on $r = 0$. The other constants $C_2(x)$ and $C_4(x)$ are determined using (2.17), (2.18) and the solutions are given by

$$V_x = -1 + \frac{1-N}{2(2-N)}\frac{dp}{dx}\left[r^2 - h^2 + \frac{Nh}{m}\left(\frac{I_0(mh) - I_0(mr)}{I_1(mh)}\right)\right], \tag{3.6}$$

$$v_\theta = \frac{1-N}{2(2-N)}\frac{dp}{dx}\left[\frac{hI_1(mr)}{I_1(mh)} - r\right]. \tag{3.7}$$

From (3.7), we observe that $v_\theta = 0$ on $r = 0$ as we expect microrotation to become zero on the axis, Eringen [7]. The corresponding stream function ($V_r = -\frac{1}{r}\frac{\partial\psi}{\partial x}$ and $V_x = \frac{1}{r}\frac{\partial\psi}{\partial r}$) is

$$\psi = -\frac{r^2}{2} + \frac{1-N}{2(2-N)}\frac{dp}{dx}\left[\frac{r^4}{4} - \frac{h^2r^2}{2} + \frac{Nh}{mI_1(mh)}\left(\frac{r^2I_0(mh)}{2} - \frac{rI_1(mr)}{m}\right)\right] \tag{3.8}$$

The dimensionless flux ($q = q'/\pi a^2 c, q'$ being the flux in the wave frame) is given by

$$q = \int_0^h 2rV_x dr = -h^2 - \frac{1-N}{4(2-N)}\frac{dp}{dx}[h^4 + f(h)], \tag{3.9}$$

where

$$f(h) = \frac{4Nh}{m}\left[\frac{(h/m)I_1(mh) - (h^2/2)I_0(mh)}{I_1(mh)}\right]. \tag{3.10}$$

The pressure gradient is obtained from Eq. (3.9) as

$$\frac{dp}{dx} = -\frac{4(2-N)}{(1-N)}\left[\frac{q+h^2}{h^4 + f(h)}\right]. \tag{3.11}$$

Integrating (3.11) over one wave length, we get

$$\Delta p = p_1 - p_0 = -\frac{4(2-N)}{(1-N)}(qL_1 + L_2), \tag{3.12}$$

where

$$L_1 = \int_0^1 \frac{dx}{h^4 + f(h)} \quad \text{and} \quad L_2 = \int_0^1 \frac{h^2dx}{h^4 + f(h)}.$$

The physical quantity of interest, the nondimensional time averaged flux $\bar{Q}$ over one period in the fixed frame of reference [1], is

$$\bar{Q} = \frac{1}{T}\int_0^T (q + h^2)dt = q + q_1, \tag{3.13}$$

where $q_1 = \int_0^1 h^2 dx$. From (3.12) and (3.13), the relation between Δp and $\bar{Q}$ is obtained as

$$\Delta p = -\frac{4(2-N)}{(1-N)}\left[(\bar{Q} - q_1)L_1 + L_2\right]. \tag{3.14}$$

Equation (3.14) is rewritten in the form:

$$\bar{Q} = q_1 - \frac{L_2}{L_1} - \left[\frac{1-N}{4(2-N)}\right]\frac{\Delta p}{L_1}. \tag{3.15}$$

In the limit of micropolar parameter $N \to 0$, (3.14) and (3.15) reduce to the corresponding relations for a viscous fluid given by Shapiro et al. [1].

4 Discussion of the results

4.1 Pumping characteristics

Pumping characteristics are analyzed by choosing three types of nondimensional wave forms, namely sinusoidal, expansion (+sign) and contraction (−sign) waves, given by

$$h(x) = 1 + \phi\, sin(2\pi x) \quad 0 \le x \le 1, \tag{4.1}$$

$$\left.\begin{aligned} h(x) &= 1 \pm \phi\, sin(\pi x/\lambda_c) && 0 \le x \le \lambda_c \\ &= 1 && \lambda_c \le x \le 1 \end{aligned}\right\}, \tag{4.2}$$

where $\phi = b/a$ the amplitude ratio. The wave of expansion or contraction given by Eq. (4.2) are confined to a portion of length λ_c and remains same over the rest of the wavelength giving straight section. The expression for q_1 in (3.13) depends on the wave form one chooses. When pressure difference $\Delta p = 0$, (i.e $p(1) = p(0)$) which is called free pumping and the corresponding time average flux is denoted by $\bar{Q}_0$. The maximum pressure against which the peristalsis works as a pump i.e Δp corresponding to $\bar{Q} = 0$ is denoted by P_0. When $\Delta p < 0$, the pressure assists the flow and it is known as copumping. The integrals L_1 and L_2 in (3.15) are evaluated using a numerical quadrature of Matlab package.

The variation of Δp with $\bar{Q}$ for the waveform given by (4.1) with $\phi = 0.4, m = 2.0$ for different values of N is shown in Fig. 1. It is observed that the pumping region ($0 \le \Delta p \le P_0$) increases as the coupling number N increases and $N = 0$ corresponds to the case of Newtonian fluid. It appears from Fig. 1a that free pumping is independent of N but it is not true as seen from the enlargement shown in Fig. 1b. It is interesting to note that the lines for different values of N intersects in the region $\Delta p < 0$. Figure 2 depicts the pressure gradient Δp versus $\bar{Q}$ with $\phi = 0.4$, $N = 0.8$ and for different values of the micropolar parameter m. Here, we observe the pumping region increases with decreasing m and greater than the case of a Newtonian fluid. The enlargement of the free pumping in Fig. 2b indicates that the lines for different m intersect in a narrow region around $\Delta p = 0$. Thus, there is no considerable difference in free pumping flux for Newtonian or micropolar fluids but the peristalsis in micropolar fluids works as a pump against greater pressure rise compared to Newtonian fluid. similar results were observed by [10, 11] when couple stresses are taken into account in the fluid model.

Provost and Schwarz [3] have observed an interesting phenomena in free pumping for a certain non-Newtonian (Reiner-Philippoff) fluid model that the mean flow rate is zero or negative for a straight section dominated (SSD) expansion or contraction waves similar to ones given in (4.2) and stressed the importance of wave shape in peristaltic transport. In what follows, we have examined whether this type of result is possible in the case of micropolar fluids. For the wave shape given in (4.2) for expansion and contraction waves with $\phi = 0.4$ and $\lambda_c = 0.3$ we have plotted the variation of Δp with $\bar{Q}$ for different values of N and m in Figs. 3

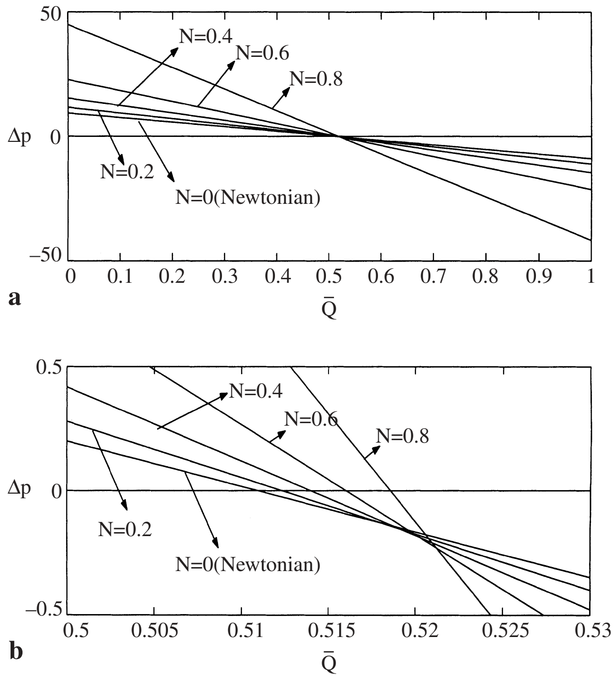

Fig. 1. Variation of Δp with $\bar{Q}$ for sinusoidal wave with $\phi = 0.4$ and $m = 2.0$; **a** for different values of N, and **b** enlargement of the free pumping region ($\Delta p = 0$)

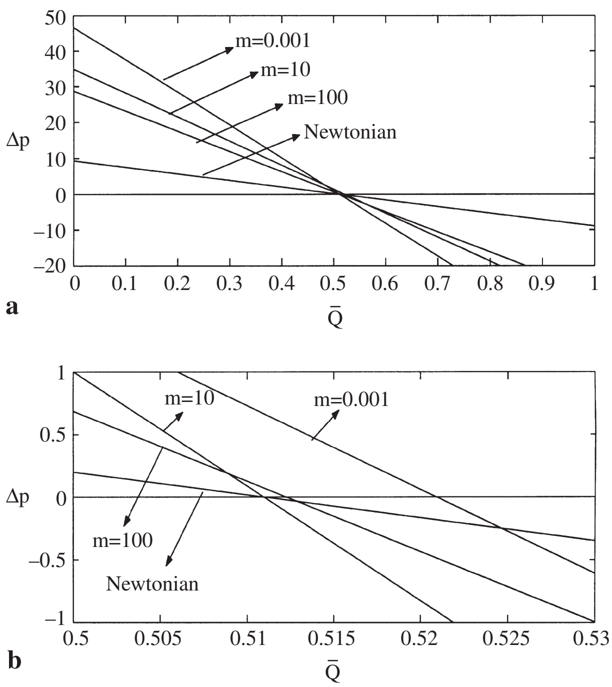

Fig. 2. Variation of Δp with $\bar{Q}$ for sinusoidal wave with $\phi = 0.4$ and $N = 0.8$; **a** for different values of m, and **b** enlargement of the free pumping region ($\Delta p = 0$)

and 4, respectively. It is seen from the figures that the time mean flow rate is always positive for all favourable pressure differences in pumping region and never goes to the third quadrant as observed by [3, 5] for any choice of m and N. This is not surprising as $\bar{Q}$ for micropolar fluids with any m and N is always greater than that of a Newtonian fluid.

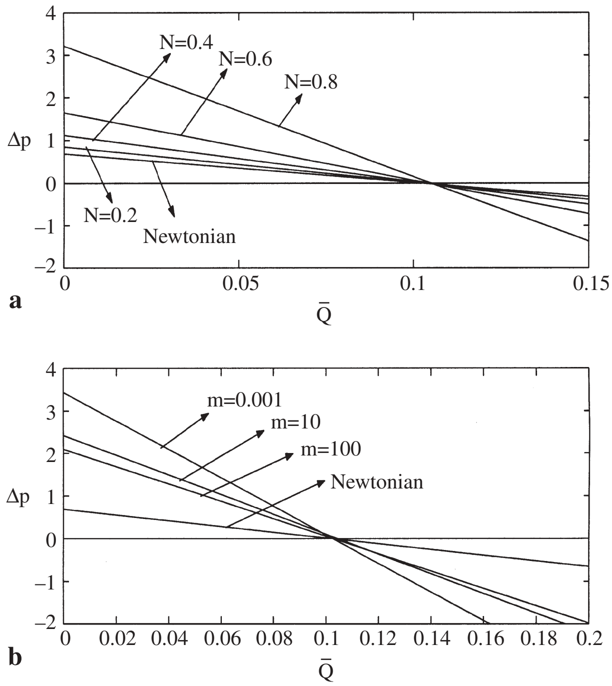

Fig. 3. Variation of Δp with $\bar{Q}$ for the expansion wave with $\phi = 0.4$, $\lambda_c = 0.3$; **a** $m = 2.0$ for different values of N, **b** $N = 0.8$ and for different values of m

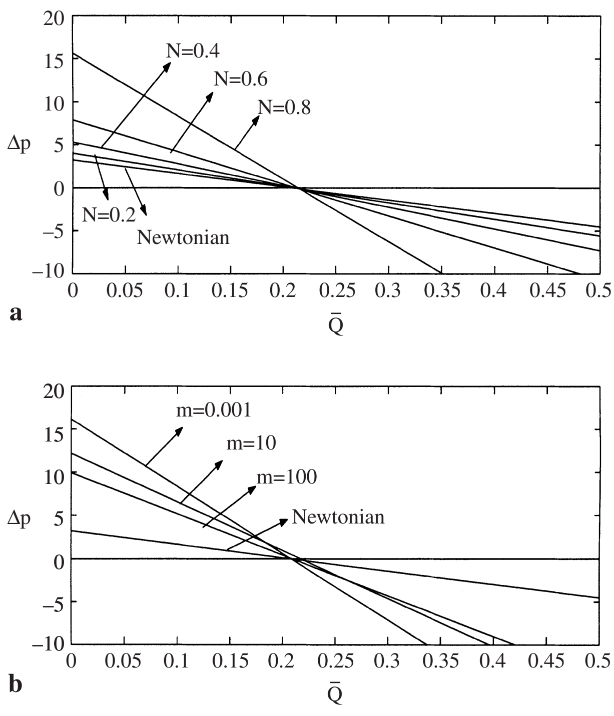

Fig. 4. Variation of Δp with $\bar{Q}$ for the contraction wave with $\phi = 0.4$, $\lambda_c = 0.3$; **a** $m = 2.0$ for different values of N, **b** $N = 0.8$ and for different values of m

4.2 *Friction force*

It is very interesting to note that for fluids in microcontinum (couple stress fluids, micropolar fluids, polar fluids, dipolar fluids, etc) the stress tensor is not symmetric. The nonzero dimensionless shear stresses in our problem are given by

$$\tau_{zr} = \frac{\partial V_x}{\partial r} - \frac{N}{1-N} v_\theta, \tag{4.3}$$

$$\tau_{rz} = \frac{1}{1-N}\frac{\partial V_x}{\partial r} + \frac{N}{1-N} v_\theta. \tag{4.4}$$

Now, the dimensionless friction force F_1 on the inner wall of the tube using (4.3) over one wavelength is (see Bird et al. [17]).

$$F_1 = -2\int_0^1 h(x)(\tau_{zr})_{r=h(x)} dx = -2\int_0^1 h(x)\left(\frac{\partial V_x}{\partial r}\right)_{r=h(x)} dx, \tag{4.5}$$

as $v_\theta = 0$ at $r = h(x)$. Substituting for V_x from (3.6) in (4.5) and using (3.11), (3.15) after some simplification, we get

$$F_1 = -(1-N)\int_0^1 h^2 \frac{dp}{dx} dx = 4(2-N)\left(L_3 - \frac{L_2^2}{L_1}\right) - (1-N)\Delta p \frac{L_2}{L_1}, \tag{4.6}$$

where $L_3 = \int_0^1 \frac{h^4 dx}{h^4 + f(h)}$.

Similarly, using the other expression τ_{rz} we get the frictional force as

$$F_2 = -\int_0^1 h^2 \frac{dp}{dx} dx. \tag{4.7}$$

The nondimensional friction force F_1 given in (4.6) is numerically calculated for a sinusoidal wave as a function of ϕ for different m and N in pumping, copumping and free pumping cases and is presented in Fig. 5. Figure 5a shows the variation of F_1 with $m = 10$ for a different values of N in free pumping ($\Delta p = 0$) and copumping ($\Delta p = -2.0$) cases. It is observed that the friction force reduces with increasing N but it increases with increasing ϕ. Further, we observe that the friction force for a Newtonian fluid is always greater than that for a micropolar fluid. Similar things are observed for fixed N and different m as shown in Fig. 5c. When $\phi = 0$, friction force depends on N only but not on m in pumping and copumping ranges as seen from Fig. 5. However, we observe some interesting feature in pumping case namely the friction force increases with increasing N near $\phi = 0$ where as opposite happens near $\phi = 0.9$ as depicted in Fig. 5b. Many authors dealing with fluids of microcontinum like Srivastava [10], Philip and Peeyush [11], etc. have discussed the frictional force given by F_2 in (4.7) only. The frictional force F_2 calculated from (4.7) for different value of N is shown in Fig. 5d. Here we observe that the friction force increases with the micropolar parameter N as well as with ϕ in all pumping ranges of pressure gradient. The friction force for a Newtonian fluid is always less than that for a micropolar fluid. This is similar to the observation of Srivastava [10] for the couple stress fluid. The only nonzero microrotation component v_θ gives rise to stress couple components $m_{r\theta}$, and $m_{\theta r}$. It is observed that they do not contribute to peristaltic pumping and therefore are not studied here.

4.3 *Trapping phenomena*

Another interesting physical phenomena of peristalsis is trapping, the formation of an internally circulating bolus of fluid which moves along with the wave. The presence of center line

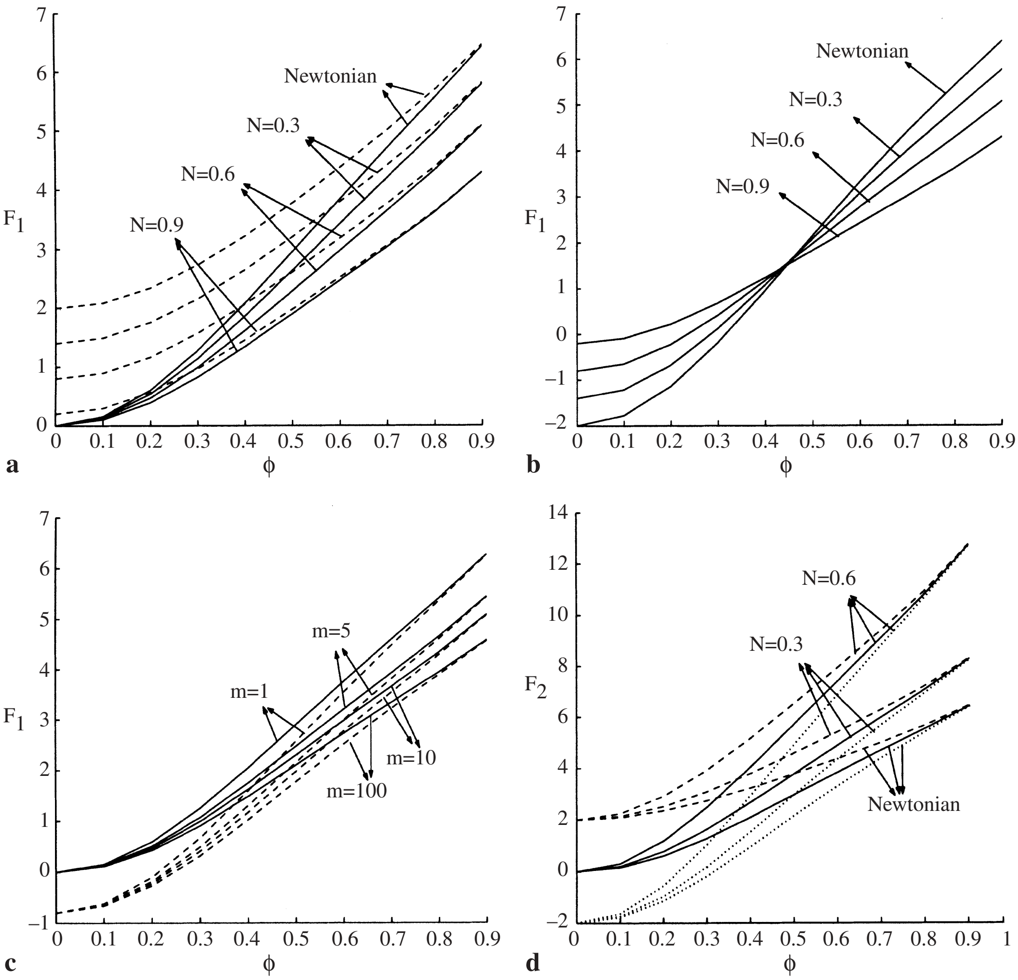

Fig. 5. Variation of friction force F_1 with amplitude ratio ϕ; **a** with $m = 10$ for different values of N $\Delta p = 0$ (solid line, free pumping) and $\Delta p = -2.0$ (dash line, copumping), **b** with $m = 10$ for different values of N, $\Delta p = 2.0$ (pumping) and **c** with $N = 0.6$ for different values of m for $\Delta p = 0$ (solid line) and 2.0 (dash line), **d** variation of friction force F_2 with ϕ for $m = 10$ and $\Delta p = 0$ (solid line), $\Delta p = -2.0$ (dash line) and $\Delta p = 2.0$ (dotted line)

trapping is the existence of stagnation points in the wave frame which can be located at the intersection of both velocity component ($V_x = 0$ and $V_r = 0$) and center line $r = 0$. From Eqs. (3.6) and (3.11), the stagnation points are given by

$$V_{x|r=0} = -1 - 2\frac{(\bar{Q} - 1 - \frac{\phi^2}{2} + h^2)}{h^4 + f(h)}\left[-h^2 + \frac{Nh}{m}\left(\frac{I_0(mh) - 1}{I_1(mh)}\right)\right] = 0, \tag{4.8}$$

as $V_r = 0$ at $r = 0$. This implies

$$\bar{Q} = 1 + \frac{\phi^2}{2} - h^2 + \frac{h^2 + f(h)}{2\left[h^2 - \frac{Nh}{m}\left(\frac{I_0(mh)-1}{I_1(mh)}\right)\right]}. \tag{4.9}$$

We consider here the trapping phenomena only for the sinusoidal wave form. The stagnation points are real if the roots of Eq. (4.8) satisfy [16],

$1 - \phi \leq h \leq 1 + \phi$.

By analyzing from Eq. (4.9), one gets the trapping when $\bar{Q}$ lies between

$$Q_L \leq \bar{Q} \leq Q_M, \tag{4.10}$$

where $Q_L = \bar{Q}|_{h=1+\phi}$ and $Q_M = \bar{Q}|_{h=1-\phi}$. The lower limit ($Q_L$) and upper limit ($Q_M$) are always less than the corresponding limits for the Newtonian fluid and lie in the pumping region. Further, in the limit $N \to 0$, they reduce to the Newtonian fluid case.

Figure 6 illustrates the streamline pattern for different values of N with $m = 2.0$, $\phi = 0.4$, $\bar{Q} = 0.1$. It is observed that the size of the trapping bolus increases as N increases. There is no trapped bolus for $N = 0$ Fig. 6a, as the flux $\bar{Q} = 0.1$ is less than the lower trapping limit for a Newtonian fluid where as it lies within the limit of trapping for a micropolar fluid. Streamlines for $\bar{Q} = 0.25$ with $m = 2.0$, and $\phi = 0.4$ are plotted in Fig. 7. We observe the trapping bolus shifting towards the boundary wall as the flux $\bar{Q} = 0.25$ lies in the copumping region and this is similar to the observation made by Ramachandra Rao and Usha [18]. Here also the effect of N on trapping is same as in the copumping case namely the size of trapped region increases with increasing N. The effects of micropolar parameter m on the trapping with fixed values of $N = 0.8, \phi = 0.4$ and $\bar{Q} = 0.1$ are shown through the streamline patterns in Fig 8. It is

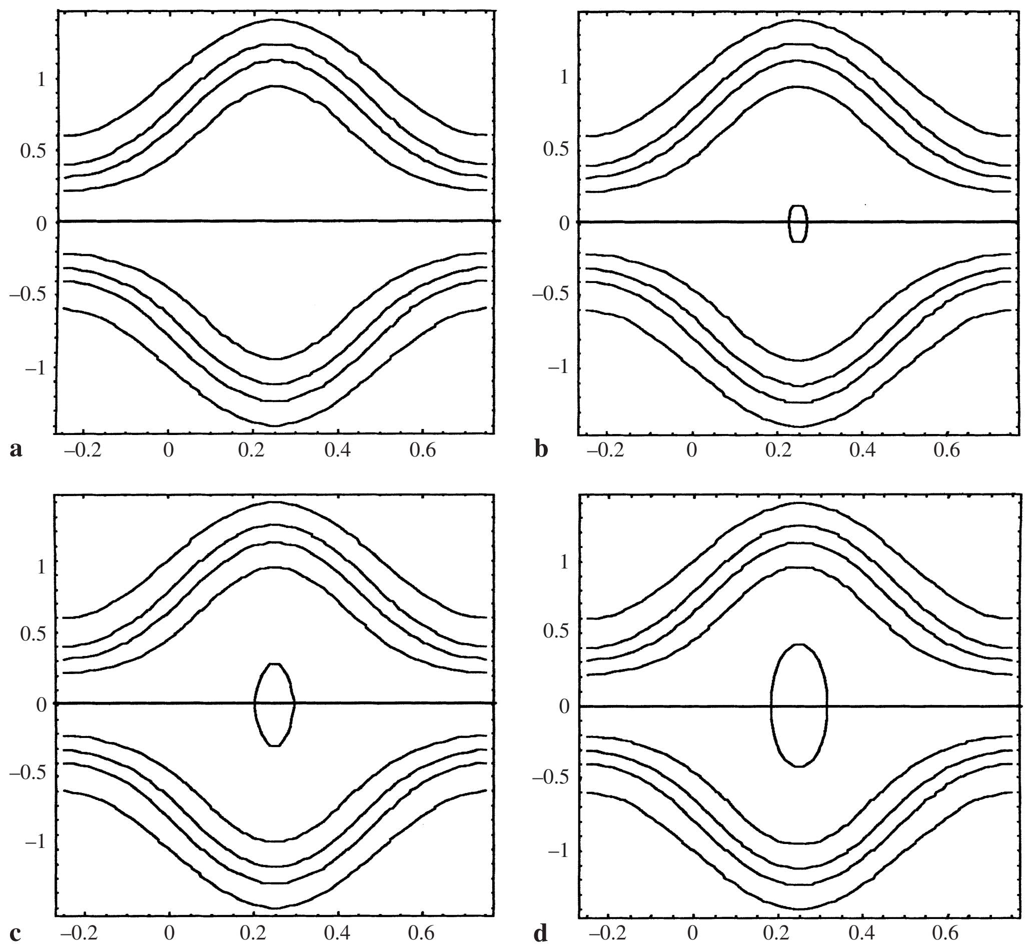

Fig. 6. Streamlines for $m = 2.0, \phi = 0.4$ and $\bar{Q} = 0.1$; **a** $N = 0$, **b** $N = 0.1$, **c** $N = 0.4$, and **d** $N = 0.8$

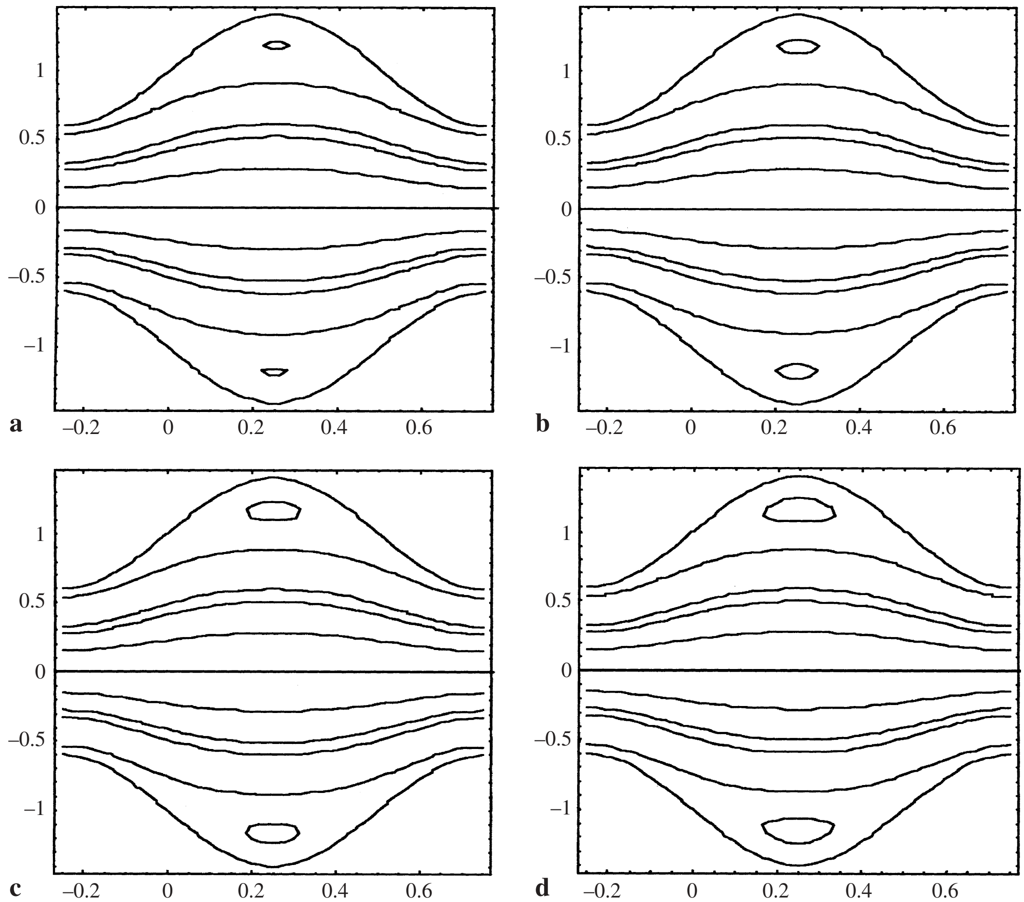

Fig. 7. Streamlines for $m = 2.0, \phi = 0.4$ and $\bar{Q} = 0.25$; **a** $N = 0$, **b** $N = 0.3$, **c** $N = 0.6$, and **d** $N = 0.9$

interesting to observe that the trapped bolus size increases with m upto a certain value of m and shows incipient decrease later. As the value of $\bar{Q} = 0.1$ is chosen to lie outside the limit of center streamline trapping, we do not see any trapping in Fig 8a.

5 Conclusions

A mathematical model on peristaltic pumping of an incompressible micropolar fluid is analyzed in the waveframe of reference with the assumptions of long wavelength and zero Reynolds number. It is interesting to observe that the pumping is improved for all choice of parameters for a micropolar fluid compared to Newtonian fluid. As it is speculated that blood flow in vasomotion is by peristalsis, modeling of blood in these vessels by a micropolar fluid is better. Recently, it is noticed that in the transport of grannular material the couple stresses play an important role [19], [20]. Provost and Schwarz [3] predicted that any deviation from Newtonian fluid allows one to find at least one non-trivial waveform for which the time mean flow rate is zero or negative for a favorable pressure gradient. But for a micropolar fluid we observe that the time mean flow rate does not follow the predictions made by [3] for the micropolar parameters considered. The limits on mean flow rate on the

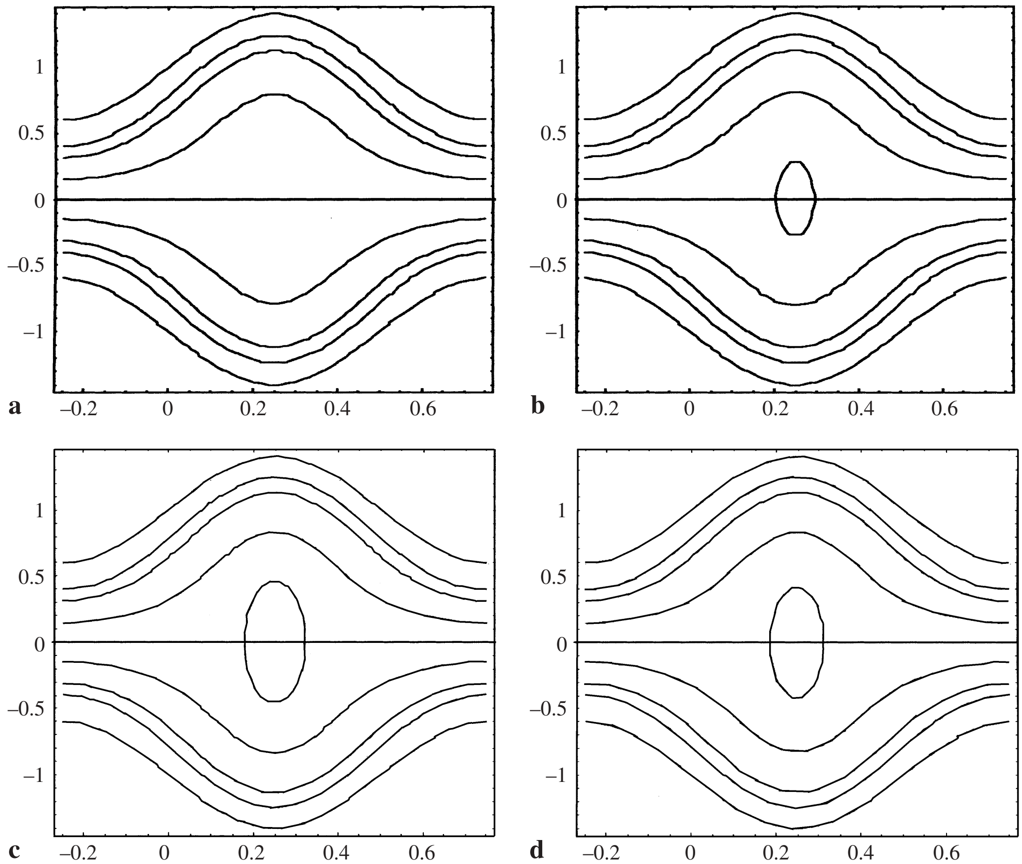

Fig. 8. Streamlines for $N = 0.8, \phi = 0.4$ and $\bar{Q} = 0.1$; **a** $m = 0.1$, **b** $m = 1$, **c** $m = 7$, and **d** $m = 10$

center streamline trapping is obtained and the interesting phenomena is that the micropolar parameters increase the size of the trapped bolous. The micropolar parameter effects on friction forces are discussed.

Acknowledgements

The authors thank the referees for pointing out some mistakes in the governing equations and for the suggestions to improve the presentation of the paper.

References

[1] Shapiro, A. H., Jafrrin M. Y., Weinberg, S. L.: Peristaltic pumping with long wavelength at low Reynolds number. J. Fluid. Mech. **37,** 799–825 (1969).
[2] Fung, Y. C., Yih, C. S.: Peristaltic transport. Trans. ASME, J. Appl. Mech. **35,** 669–675 (1968).
[3] Provost, A. M., Schwarz, W. H.: A theoretical study of viscous effects in peristaltic pumping. J. Fluid. Mech. **279,** 177–195 (1994).
[4] Srivastava, L. M., Srivastava, V. P.: Peristaltic transport of power law fluid: application to the ductus of efferuntus of the reproductive tract. Rheol. Acta. **27,** 428–433 (1988).

[5] Usha, S., Ramachandra Rao, A.: Peristaltic transport of two layered power law fluid. Trans. ASME, J. Biomech. Engg. **119,** 483–488 (1997).
[6] Böhme, G., Friedrich, R.: Peristaltic flow of viscoelastic liquids. J. Fluid Mech. **128,** 109–122 (1983).
[7] Eringen, A. C.: Theory of micropolar fluids. J. Math. Mech. **16,** 1–16 (1966).
[8] Ariman, T., Turk, M. A., Sylvester, N.: Application of microcontinum fluid mechanics. Int. J. Engg. Sci. **12,** 273–293 (1974).
[9] Lukaszewicz, G.: Micropolar fluids – theory and applications. Birkhäuser: Boston 1999.
[10] Srivastava, L. M.: Peristaltic transport of a couple stress fluid. Rheol. Acta. **25,** 638–641 (1986).
[11] Philip, D., Peeyush Ch.: Peristaltic transport of a simple micro fluid. Proc. Nat. Acad. Sci. India. **65(A),** 63–74 (1995).
[12] Girija Devi, R., Devanathan, R.: Peristaltic motion of a micropolar fluid. Proc. Indian Acad. Sci. **81(A),** 149–163 (1975).
[13] Muthu, P., Rathish Kumar, B. V., Peeyush Ch.: On the influence of the wall properties in the peristaltic in the peristaltic motion of micropolar fluid. ANZIAM (forthcoming)
[14] Antanovskii, L. K., Ramkissoon, H.: Long-wave peristaltic transport of a compressible viscous fluid in a finite pipe subject to a time-dependent pressure drop. Fluid Dyn. Res. **19,** 115–123 (1997).
[15] Cowin, S. C.: Polar fluids. Phys. Fluids **11(9),** 1919–1927 (1968).
[16] Jaffrin, M. Y.: Inertia and streamline curvature effects on peristaltic pumping. Int. J. Engng. Sci. **11,** 681–699 (1973).
[17] Bird, R. B., Stewart, W. E., Lightfoot, E. N.: Transport phenomena. New York: Wiley 1960.
[18] Ramachandra Rao, A., Usha, S.: Peristaltic transport of two immiscible viscous fluids in a circular tube. J. Fluid Mech. **298,** 271–285 (1995).
[19] Srinivasa Mohan, L., Kesava Rao, K., Nott, Prabhu R.: A frictional Cosserat model for the slow shearing of granular materials. J. Fluid Mech. **457,** 377–409 (2002).
[20] Tomantschger, K. W.: A boundary value problem in the micropolar theory. ZAMM **82,** 421–422 (2002).

Authors' addresses: D. Srinivasacharya, Department of Mathematics and Humanities, Regional Engineering College, Warangal – 506 004, India (E-mail: dsc@recw.ernet.in); Manoranjan Mishra and Ramachandra Rao Adabala, Department of Mathematics, Indian Institute of Science, Bangalore – 560012, India (E-mails: mishra@math.iisc.ernet.in; ramchand@math.iisc.ernet.in)